

# Optimised Computational Functional Imaging for Arteries

Ramiro Moreno<sup>1</sup>, Ming Chau<sup>3</sup>, Shirod Jeetoo<sup>1</sup>, Franck Nicoud<sup>2</sup>, Frédéric Viart<sup>3</sup>, and Hervé Rousseau<sup>1</sup>

<sup>1</sup> Institut de Médecine Moléculaire de Rangueil (I2MR),  
CHU de Rangueil, Toulouse, France  
`moreno.r@chu-toulouse.fr`.

<sup>2</sup> Institut de Mathématiques et Modélisations de Montpellier (I3M),  
Université de Montpellier II, France

<sup>3</sup> Advanced Solution Accelerator (ASA), Montpellier, France

**Abstract.** The general framework of the Optimised Computational Functional Imaging for Arteries (OCFIA) program is to introduce high-performance scientific computing in the medical domain with the aim to rationalize therapeutic decisions in respect to vascular diseases yet poorly understood. More precisely, it consists in coupling medical imaging techniques, essentially morphological, with scientific computing, through Computational Fluid Dynamics (CFD), to yield functional imaging, thus providing to physicians a better quantitative knowledge of the biomechanical state (field of speeds, pressure, wall and Stent Graft loads ...) to the patients.

## 1 Introduction

Risk factors for cardiovascular disease (hypertension and high cholesterol) and their role have been identified, but cannot explain the observed localised occurrence and the progression of the disease (stenosis, aneurysm rupture, aortic dissection). Currently, available techniques such as Computed Tomography (CT), Magnetic Resonance Imaging (MRI) and Ultrasound (US) do not allow accurate determination of the complex velocity distribution and biomechanical load on the arterial wall. Nevertheless there is not doubt that medical imaging is an essential tool for the understanding of these pathological processes. Cardiovascular disease is clearly multi-factorial and it has been shown that deviations of the normal velocity field (changes in wall shear stress) play a key role [Caro,1969]. Despite many hemodynamic studies carried out with models of arterial bifurcations, especially the carotid artery bifurcation, the precise role played by wall shear stress (WSS) in the development and progression of atherosclerosis remains unclear. Still, it is certain that the mechanical load induced by the fluid on atherosclerotic plaques and their surrounding tissues is of the utmost importance for predicting future rupture (culprit plaques) and preventing ischemic events [Corti,2002]. In the same way, the risk of rupture of an aortic abdominal aneurysm (AAA) depends more on biomechanical factors than simply on the aneurysm diameter.

Although clinical decisions are based only on the latter today, wall tension is a significant predictive factor of pending rupture [Aaron, 2000].

Computational Fluid Dynamics (CFD) techniques can provide extremely detailed analysis of the flow field and wall stress (shear & tensile) to very high accuracy. New advances in simulation techniques could make a significant contribution to a better quantitative knowledge of the biomechanical condition of the arteries and lead to a new understanding via deepened insights into these conditions. Advanced simulations could potentially be used for predicting plaque and aneurysm rupture, improving endovascular prosthesis design, as well as for guiding treatment decisions by predicting the outcome of interventional gesture (i.e. stent-coil technique).

However, applying computational fluid dynamics (CFD) to actual pathological regions of the arterial tree is very challenging and has never been done so far with sufficient accuracy and time efficiency to be useful in the clinical practice. Today's medical research is strongly linked with advances in parallel and high performance computing. Ambitious research programs such as NeuroSpin (Saclay, France) are feasible thanks to the support of the computational resources of CEA (9968, 63 TFlops, 7th in the top 500 supercomputers). Data storage, visualization and grid infrastructure are also key issues. The development of Virtual Vascular Surgery is encouraged by grid computing consortiums such as Crossgrid. There is no doubt that advances in computational resources and infrastructure will benefit to the medical community. In return, more and more challenging applications will rise and stimulate research and development.

We present a complete, optimized calculation chain whose input come from an entirely non-invasive 4D MRI protocol that provides time varying geometry and flow rates and output is a realistic functional imaging description of the arterial tree region of interest. Preliminary results were obtained through parallel computing with AVBP code (CERFACS, Toulouse, France) and classical Arbitrary Lagrangian Eulerian (ALE) formulation.

## 2 Materials and Methods

### 2.1 Image acquisition: MRI protocol

All the images were obtained with a 1.5 T MR scanner (Intera; Philips Medical Systems, the Netherlands) with a 5-element phased-array coil for signal reception (Sense Cardiac, Philips Medical Systems).

The objective of following processing steps was to translate the image data set into patient-specific conditions (boundary conditions) suitable for CFD calculations.

**MR Angiography** The routine injected (Gd-DTPA, Magnevist, Schering, volume injected 20mL, injection rate 5mL/s) T1-Full Field Echo sequence was performed on sagittal-oblique planes, parallel to the major aortic axis, in order to cover the whole aorta geometry (field of view, 450x450x126mm) with a spatial

resolution of  $0,88 \times 0,88 \times 1,80 \text{mm}^3$ . This acquisition was triggered to the patient ECG, 430ms after the R wave (diastolic phase).

**Single Slice 2D MR Cine Imaging** A dynamic balanced Steady State Free precession (b-SSFP) sequence, was performed on transverse planes, to cover the thoracic aorta and segment the cardiac cycle in 20-40 phases.

**MR flow quantification** 2D Phase-Contrast (PC) sequences, performed orthogonal to the vessel axis, provided the velocity inlet profiles at the ascending, descending aorta, and supraaortic vessels. Supplementary transversal-oblique and sagittal-oblique acquisitions, respectively orthogonal to the short and long aortas axis, were performed to compare quantitatively the velocity results from the CFD.

## 2.2 Image data processing

All of the next procedures described in this chapter were developed in-house in a Matlab language (The Matlabworks, Inc) with some C compiled routines (mexfiles) integrated to main sources. Some of them (affine coregistration and high dimensional warping are initially developed by John Ashburner into SPM (statistical parametric mapping toolbox University College London, 2000), an image processing toolbox dedicated to computational neuroanatomy. The images were initially obtained in DICOM format and were converted to the Analyze-7 format (Mayo Clinic, Rochester, USA., <http://www.mayo.edu/bir/>) for filtering and non-linear-transformation operations. The meshes were initially built in an ASCII format (\*.cas) into the Amira 4.1 environment (TGS, Mercury Computer Systems, USA). The final set of moving meshes and hemodynamic boundary conditions are exported into the correct AVBP format (CERFACS, Toulouse, France, <http://www.cerfacs.fr>) in order to perform CFD runs. Finally, all post-processing steps before CFD step were operated with a Pentium(R) Duo 3,4 GHz processor with 1.5Go RAM. The geometrical post-processing operations are highlighted on the figure 1.

**Filtering** MR image noise affects the post-processing algorithms. Filtering can be used to limit image noise but current filters reduce spatial resolution. In this work we applied a selective blurring filter to anatomical MR data. The filtered static data acquisition are submitted to 3D Level Set algorithm (see section Initial Mesh) for a segmentation step. Compared to other classical filters, this filter achieves the best compromise between spatial resolution and noise reduction [Gensanne, 2005]. The homogeneous regions must have the same gray level, so if the noise (gradient) is less than  $2 \times \text{SNR}$  (95%), the selective blurring filter apply a hard smooth (weighting=1). The treatment is different for the fine details where gradient is greater than  $2 \times \text{SNR}$  the filter gradually weight the smooth according to the image neighbours gradient (weighting= $1/\text{gradient}$ ).

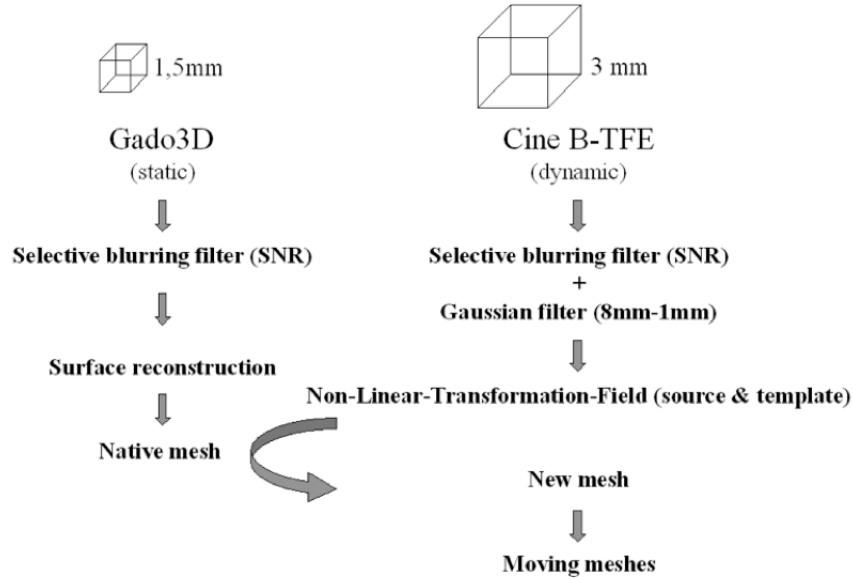


**Fig. 1.** Postprocessing steps for moving mesh preparation from MRI acquisitions

**Initial Mesh** After this stage of filtering, the anatomical surface can be extracted by means of level-set/fast marching methods [Sethian, 1999] that accurately model the complex surfaces of pathological objects. With the static geometry acquisition, the level set methods offer a highly robust and accurate method for tracking the interface in a volume of interest coming from the static and contrast-enhanced MRI acquisition.

Given an initial position for an interface  $\gamma_0$  (endovascular surface), where  $\gamma$  is a closed surface in  $R^3$ , and a speed function  $F$  which gives the speed of  $\gamma$  in its normal direction, the level set method takes the perspective of viewing  $\gamma$  as a zero level set of a function  $\phi$  from  $R^3$  to  $R$  whose evolution equation is eq. 1 and where  $\phi$  represents the distance function.

$$\begin{cases} \phi_t - F|\nabla\phi| = 0 \\ \phi(x, t = 0) = \pm d(x) \end{cases} \quad (1)$$

The filtered static data acquisitions (T1-Full Field Echo sequences) are submitted to the in-house 3D Level Set algorithm for a fine geometrical extraction step (Matlab 7.0, the MathWorks, Inc). An initial computational grid was obtained by the discretization of this geometry (Amira 4.1).

**Moving Mesh** Wall movements were imposed to the initial grid according to cine scan acquisition (b-SSFP), by means of the non linear transformation field algorithm of SPM-2 toolbox (Matlab 7.0, the MathWorks, Inc). A tetraedral

moving grid was built [Moreno, 2006] according to estimated non-linear deformation fields (Fig. 2 shows the mesh and its deformation on a section). Each phase of the transformation process consists in estimating the deformation between the native and a target image. Therefore, the whole transformation is completed when the deformations to all the target images of a cardiac cycle are computed. The meshes used at each time step of CFD simulation are obtained by applying the computed deformation (according to cine scan images) to the native mesh (obtained from injected sequence).

Specifically, the optimization approach is used here. We are trying to find the best compromise between effective transformation, by a function  $F_2$  (eq.3), and regular transformation, by a function  $F_1$  (eq.2) which corresponds to the sum of local volume variations ( $\frac{\Delta V}{V} = |J| - 1$ ). The deformation gradient tensor  $J$  is computed according to the coordinates of  $T(x)$ . Optimization process consists in finding  $T$  which minimizes a linear combination of  $F_1$  and  $F_2$  (eq.4).

$$F_1 = \int_{\Omega} (|J| - 1) d\Omega + \int_{\Omega} (|J|^{-1} - 1) d\Omega \quad (2)$$

$$F_2 = \int_{\Omega} [I_{source}(x) - I_{target}(T(x))]^2 d\Omega \quad (3)$$

$$F = \lambda F_1 + F_2 \quad (4)$$

The derivative of  $F$  is computed with symbolic calculation tool and a gradient algorithm is used. The phases of the transformation process (Fig. 2) can be computed independently. This is a straightforward parallelization.

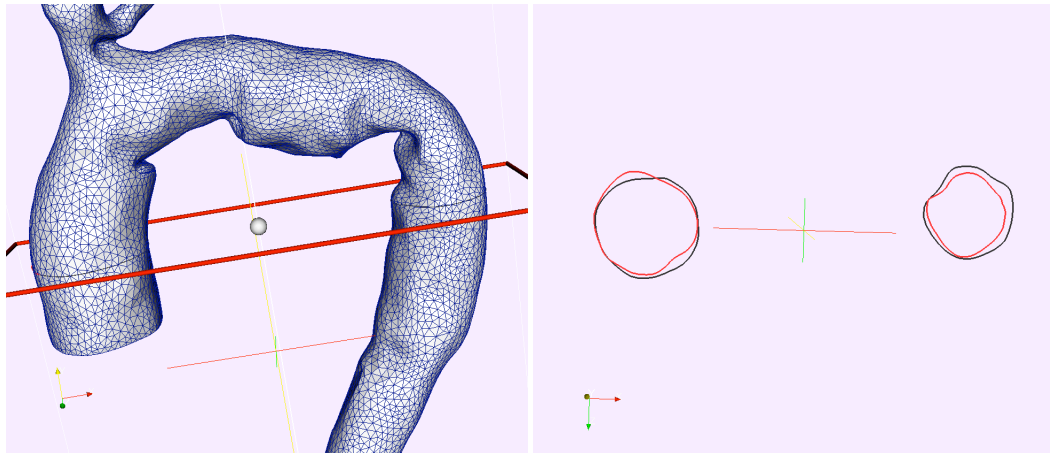


**Fig. 2.** Moving meshes (2 cardiac phases)

**Hemodynamic Boundary Conditions** A region of interest (ROI) defined the vascular area on the Phase Contrast (PC) quantitative images to extract velocity data samples. A curve fitting calculation was applied to this data set using the general Fourier model in order to obtain a time-dependent function. This process was applied to all the orthogonal sections to the short aorta axis (Fig. 3). The areas corresponding to the ascending, descending aorta and supraaortic vessels provided inlet and outlet conditions for CFD, while the mid descending aorta was used for the control. The arrow on the right side image points out a strongly turbulent flow. Note that these MRI images give the vertical component of velocity.



**Fig. 3.** Phase contrast acquisition for the inlet/outlet velocity evaluation

### 2.3 CFD application

A first numerical model was developed [Nicoud, 2005] in order to assess the wall shear stress changes after endovascular stenting. In this approach, the fully coupled fluid–structure problem is replaced by a simpler fluid problem with moving boundaries. The NavierStokes equations were solved numerically with an appropriate finite-element-based method which handles time-dependent geometries. The main result supports the idea that stenting can induce endothelial dysfunction via haemodynamic perturbations. From this study, which enabled us to check the feasibility of an uncoupled CFD, we widened the problem with the more complex case of vascular geometries.

The flow simulations were performed using the finite volume (FV) method, as implemented in the AVBP code (CERFACS, European Center for Research and Advanced Training in Scientific Computation, Toulouse, France).

The FV method used in the code solves the full Navier-Stokes equation, who governs the flow, by an efficient explicit Arbitrary Lagrangian Eulerian (ALE) formulation (Fig. 4), which allows to impose the tetraedral moving grid within cardiac cycles.

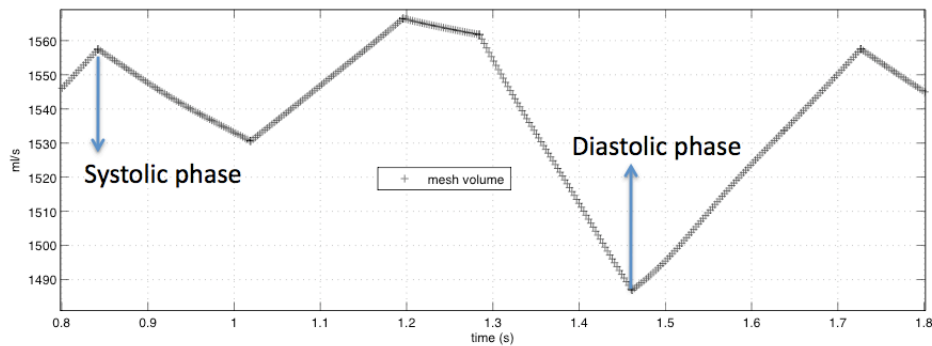


**Fig. 4.** Total mesh volume : run process (one ALE run per cardiac phase) for HPC

Hemodynamic conditions (time-dependent functions) were synchronized with the wall motion and were imposed in the form of speed profiles at the entry (ascending aorta) and exit (descending aorta, supraortic vessels) of the numerical field (aorta district). Blood was assumed to be a homogeneous newtonian fluid with a dynamic viscosity approximated as 4 cPoi and a density of 1050 kg/m<sup>3</sup> (physiologic blood value in aorta and collaterals). The simulations began from an initially quiescent flow state and continued for a number of full cardiac cycles in order to allow the development of a fully periodic flow, representative of a regular heartbeat. It was found that the main features of the vascular flow field became stable within four cycles.

Uncoupled CFD results were performed in HPC system (IBM, Power4, Cines, Montpellier, France) and were controlled by the additional MRI quantitative-flow-imaging performed at intermediate levels during the examination. Geometric deformation field was validated by 3D visual correlation between moving mesh and cine scan imaging.

Tetraedral Grid Resolution (minimum length: 1mm; maximum length 2.3 mm), balanced between the grid independence and time efficiency conditions, was sufficient for preliminar results on Carotid Bifurcation and Thoracic Aorta CFD calculations.

### 3 Results

Thoracic aorta studies were performed in both volunteers and patient cases (Fig.5). Boundary conditions were flow controlled and Risk Factors were observed in relation with 'hot spots' in wall stress and hemodynamic results (shear stress, velocity and vorticity). Patient data set was treated in 24 hours, according to the description of the table 1. The data processing is virtually automatic, the only manual interventions are corrections of errors of the native geometry and preparation of boundary conditions during the extraction process. Normal WSS values calculated by CFD on healthy ascending regions on patients were similar to data available on literature [Efstathopoulos, 2008] performed on healthy subjects by phase-contrast MRI flow measurements and straightforward methodologies based on Poiseuille's theory of flow. Systolic ( $0.3 \pm 0.2$  N/m<sup>2</sup> compared to  $0.4 \pm 0.2$  N/m<sup>2</sup>) and diastolic ( $0.065 \pm 0.04$  N/m<sup>2</sup> compared to  $0.11 \pm 0.07$  N/m<sup>2</sup>). The same group of patients presented abnormal WSS values on landing zones ( $+12\%$  at systole,  $+35\%$  at diastole), 'plicatures' zones ( $+38\% \pm 6\%$  at systole and  $+25 \pm 11\%$  at diastole) and collateral (neck vessels) zones ( $+6 \pm 2\%$  at systole).

**Table 1.** Time consuming for the general clinical case

Chain element process	Time consuming
MRI protocol.	30 min
Level Set geometry extraction (not parallel).	60 min
Native mesh preparation and correction (interactive, manual).	120 min
Moving mesh estimation process (not parallel).	600 min
Moving mesh estimation process (parallel@2proc).	300 min
CFD (HPC, 24 proc).	600 min
TOTAL	1410 min (23h30 min)

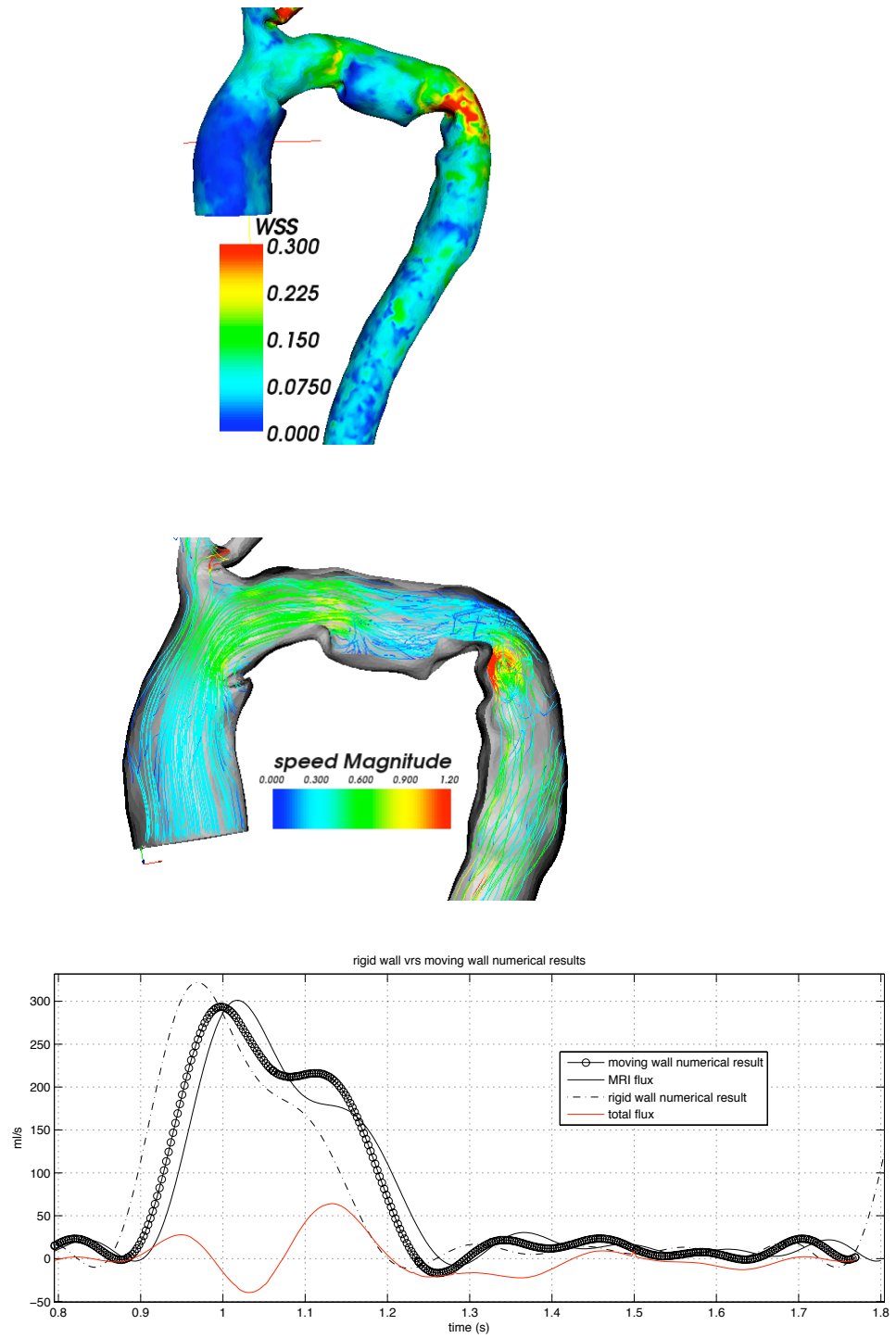


**Fig. 5.** Stented thoracic aorta : wall shear stress, stream lines velocity, control flow at intermediate level for rigid and moving wall.

**Table 2.** Run characteristics

parameter	value
number of tetraedral elements	145848
number of iterations for convergence	2.6182e+08
fixed time step for moving wall	0.55E-04 s
time step for rigid wall	0.32E-04 s
delta Volume for moving mesh	84 mL

## 4 Discussion

Following the extraction from the Level Set method, we found that it was restrictive to make weary calculations to extract the initial geometry. Sethian’s method is indeed very interesting but it depends heavily on the image quality. Partial volume artefacts increase with the thickness of the slice for a given imaging volume and results in blurring in regions where several vessels cross. An extraction method with the Level Set technique is erroneous because it sees a single vessel rather than distinguishing them. We try to solve this problem by asking experienced radiologists to make the geometry extraction through a threshold setting procedure. It revealed to be very efficient, the extraction being made instantaneously with the possibility for error correction by the user.

The flow curves obtained in the reference plan reveals the importance of taking into account the mobile wall in a realistic case. The result obtained in a rigid mesh is far better compared to the MRI measures. Yet the results obtained on a moving mesh are very similar to the control measures. It seems obvious that a realistic calculation needs to be done according to the rheology of the wall.

The calculations of deformation fields require a single pair of reference volumes (source and template). The computations have been performed on a dual-core processor (table. 1). The  $N$  deformations to be computed are dispatched on the processors. As they are independant, no communication is required during the parallel computing. It is thus trivial to reduce the time to  $1/n$  if we have such processors at our disposal.

## 5 Conclusion

The proposed approach permits the computation of the blood flow under realistic in vivo, time evolving and flow controlled conditions. It is much simpler than the full coupled fluid-structure problem and has the potential to provide a better picture of the specific hemodynamic status. The method gives a direct way to impose realistic wall interaction to hemodynamic time boundary conditions, from medical examinations performed into a simple MR protocol. A future improvement in the processing chain described in this work will facilitate biomechanical functional imaging in less than 8 hours, which would be useful

for clinical practice. Insights about the physiopathology of some arterial diseases and endovascular treatment are also expected.

## References

- [Caro,1969] Caro, C., Fitz-Gerald, J., Schroter, R.: Arterial wall shear and distribution of early atheroma in man. *Nature* 211. **223** (1969) 1159–1160.
- [Corti,2002] Roberto Corti, MD, Lina Baldimon, PhD, Valentin Fuster, MD, PhD and Juan Jos Badimon, PhD: Endothelium, flow, and atherothrombosis, Assessing and Modifying the vulnerable atherosclerotic plaque, American Heart Association, ed Valentin Fuster (2002)
- [Aaron, 2000] Aaron J. Hall, Edward F.G. Busse, Don J. McCarville, John J. Burgess.: Aortic wall tension as a predictive factor for abdominal aortic aneurysm rupture: improving the selection of patients for abdominal aneurysm repair. *An Vasc Surg.***142** (2000) 152–157.
- [Gensanne, 2005] D Gensanne, G Josse and D Vincensini, A post-processing method for multiexponential spinspin relaxation analysis of MRI signals. *Physics in Medicine and Biology.* **50** (2005)1–18.
- [Sethian, 1999] J. A. Sethian, *Level Set Methods and Fast Marching Methods*, Cambridge University Press (1999).
- [Nicoud, 2005] F. Nicoud, H. Vernhet, M. Dauzat, A numerical assessment of wall shear stress changes after endovascular stenting, *Journal of Biomechanics.* **38** (1999) 2019–2027.
- [Efstathopoulos, 2008] Efstathios P. Efstathopoulos, George Patatoukas, Ioannis Pantos, Odysseas Benekos, Demosthenes Katritsis, Nikolaos L. Kelekis. Measurement of systolic and diastolic arterial wall shear stress in the ascending aorta, *Physica Medica* (2008).
- [Moreno, 2006] R. Moreno, F. Nicoud, H. Rousseau. Non-linear-transformation-field to build moving meshes for patient specific blood flow simulations. European Conference on Computational Fluid Dynamics, ECCOMAS CFD 2006. <http://proceedings.fyper.com/eccomas CFD2006>